The Cr-Cu (Chromium-Copper) System

51.996 63.546

By D.J. Chakrabarti and D.E. Laughlin
Carnegie-Mellon University

Equilibrium Diagram

The equilibrium diagram for the Cu-Cr system is of the eutectic type with a flat liquidus and complete miscibility in the liquid state, see Fig. 1. In contrast, the diagram proposed hitherto shows a miscibility gap in the liquid that is based on antiquated and debatable experimental evidence. The solid solution fields have restricted width. A metastable phase based on fcc Cr is most likely present. Calculations made in this review based on the experimental phase diagram and thermodynamic results confirm that the miscibility gap in the liquid lies immediately below the equilibrium liquidus and not above it.

The experimentally determined phase diagram of the Cu-Cr system has been at marked variance at the liquidus with the calculated one (based on thermodynamic modeling of the phase diagram data [77Kuz]) and with the measured (thermodynamic) activity results [82Tim]. A region of liquid immiscibility was suggested to exist in this system. The observation was based on experiments conducted more than sixty years ago that relied on materials of low purity [08Hin, 23Sie]. Calculations by [77Kuz], based on the quasiregular solution model using the experimental liquidus and (Cr) solidus data at lower temperatures, indicated the absence of such a miscibility gap and suggested, instead, a eutectic type of diagram. Also, the activity measurements of the liquid by [82Tim] indicated that a two-phase field existed between the liquid and solid Cr, and not between the two liquids. This was confirmed by the authors by optical microscopy of the solidified samples. No further investigations of this area of the phase diagram using purer materials have been reported. However, in view of the strong influence of impurities on phase stability (see below), it is highly possible that the miscibility gap observed by [08Hin] and [23Sie] was partly, if not completely, stabilized by impurities. The provisionally accepted diagram, presented in Fig. 1, therefore, is shown to be of the eutectic type with a nearly flat liquidus in the midcomposition range. Further experimental work is needed to verify this interpretation.

The equilibrium phases in the system are: (1) the liquid, L; (2) the fcc solid solution, (Cu), with maximum solubility

Fig. 1 Assessed Cu-Cr Phase Diagram with Selected Experimental Data

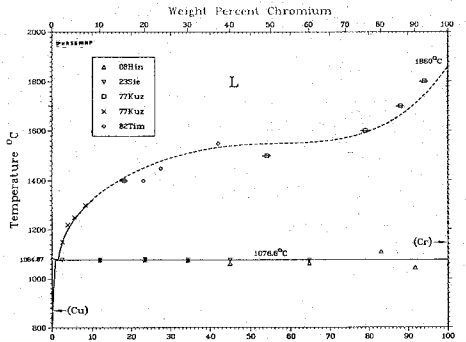

D. J. Chakrabarti and D. E. Laughlin, 1984.

of approximately 0.89 at.% Cr at 1077 °C; and (3) the bcc solid solution, (Cr), with negligible solubility of Cu below the eutectic temperature (1077 °C).

Liquidus and Solidus

Experimental data for the liquidus are available only for Cu-rich compositions. The boundaries of the liquidus in equilibrium with the (Cu) solid solution are obtained primarily from the works of [57Doi1]. The alloys were vacuum melted from high-purity Cu (99.99%) and electrolytic Cr (99% purity) and studied by thermal analysis. The temperature data taken from [57Doi1] are corrected slightly in this evaluation to conform to the accepted melting point values of Cu and Ag of 1084.87 and 961.93 °C, respectively [81BAP]. The author had used the values 1083 and 960.5 °C, respectively, for the standardization of the thermocouple. Thus, the corrected eutectic temperature comes to 1077 °C. A plot of the Cu-rich liquidus and the eutectic invariant based on the data of [57Doi1], together with the data from thermal analysis by [23Sie] and [08Hin], are shown in Fig. 2.

The Cu-rich portion of the liquidus in equilibrium with the (Cr) solid solution was determined by thermal analysis [23Sie] and by partial solute dissolution techniques [77Kuz]. The latter method was based on the isothermal equilibration of the liquid alloy and the partially dissolved Cr metal in a known charge of Cr and Cu. The composition of the liquidus was determined from the amount of undissolved Cr remaining in the (rapidly) solidified sample by its selective dissolution. The results indicated a liquidus richer in Cu than that obtained by [23Sie] (see Fig. 1 and 3).

Based on microscopy, [06Gui] inferred that Cu and Cr do not mix in the liquid, without specifying the composition range of immiscibility or the purity of the materials used. The existence of a miscibility gap in the liquid state was reported by [08Hin] and [23Sie] on the basis of thermal and microscopic work. The thermal arrest noted between 1464 and 1473 °C (Table 1) was thought to be due to the monotectic invariant temperature. The only available information on the composition range of the gap has been due to [23Sie], who estimated it to lie between 42 and 94 at.% Cr at 1467 °C (Fig. 3). The purity of the metals was very low in both the above works. The Cr used by [23Sie] was of 97.8 wt.% purity, whereas that by [08Hin] contained 1.2 wt.% Fe and 0.3 wt.% Si. The alloys of [08Hin] were also contaminated by Cr nitride, carbide, and other reaction products during melting. The effect of contamination in the Cr used by [08Hin] is evident by the large decrease in its melting point to 1550 °C, as compared to the accepted value of 1860 °C [81BAP].

It is well known that impurities often significantly affect the phase stability in alloys. This has been shown in the Cu-Nb system [78Ver, 82Cha], which is very similar to the Cu-Cr diagram at high temperatures. The Cu-Nb equilibrium diagram displays complete miscibility in the liquid state. However, a miscibility gap in the liquid can arise in this system, either by rapid cooling or by contamination with impurities, such as oxygen [78Ver]. In the former instance, the gap is in metastable equilibrium, whereas in the latter it is stabilized by the presence of the impurities.

In the Cu-Cr system the liquidus is flat in the mid-composition range, similar to that in the Cu-Nb system [82Cha], suggesting that a metastable miscibility gap is present below the liquidus. In the presence of certain impurities, it is possible that the miscibility gap is stabilized. The activity determinations on the liquid based on high-

Fig. 2 Cu-Rich Liquidus and Solidus with Selected Experimental Data

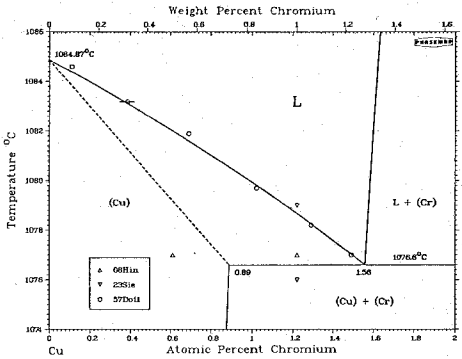

D. J. Chakrabarti and D. E. Laughlin, 1984.

Fig. 3 Calculated Liquidus and Miscibility Gap and Selected Experimental Phase Boundaries Superimposed on Assessed Diagram (Fig. 1)

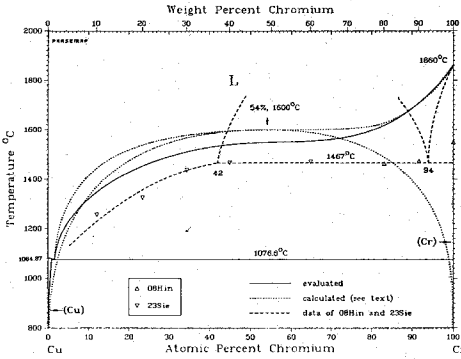

D. J. Chakrabarti and D. E. Laughlin, 1984.

purity components (99.999 wt.% Cu and 99.998 wt.% Cr) by [82Tim] indicated a gradual monotonic increase of the liquidus up to their highest measured temperature of 1616 °C. At 1550 °C, the activity of Cr, for all alloys between 42 and the highest Cr alloy used at 97 at.% Cr, was found to be constant at approximately the value of one, relative to the pure solid Cr as the standard state at that temperature. The results suggested the existence of a two-phase field between the liquid of composition 42 at.% Cr and pure solid Cr (with negligible solubility of Cu), and not between two liquids as in a miscibility gap. Microscopy on solidified samples showing the occurrence of nearly pure Cr grains supported this conclusion. Calculations made in this evaluation (see below) using the optimized thermodynamic parameters for the liquid, derived from the experimental activity results of [82Tim] and the phase diagram results of [77Kuz], confirm that the miscibility gap in the liquid lies just below the flat portion of the equilibrium liquidus (Fig. 3).

The initial slope of the liquidus at the Cr end of the diagram was calculated by the Clausius-Clapeyron equation from the freezing point depression at 1% dilution level, assuming negligible solubility of Cu in Cr. The resultant value is approximately −22.7 °C per at.% Cu. The accepted liquidus is drawn based on the data of [77Kuz] and [82Tim]. The slope of the liquidus was made to conform with the foregoing limiting slope at the Cr end. A further shift of the liquidus to higher temperatures, consistent with the calculated curve in Fig. 3 is, however, possible. Similar shifts were observed in the Cu-Nb system with the use of components of increasing purity [78Ver]. Tabulated temperature and composition data for the liquidus and solidus from different works are presented in Table 1. The corresponding data for the eutectic transformation are presented in Table 2.

Apart from the eutectic invariant, the only other available solidus data pertain to the (Cr) phase. The accepted composition (1.56 at.% Cr) and temperature (1077 °C) for the eutectic are weighted in favor of those by [57Doi1], in view of the better purity materials used and the consistent results obtained. The monotectic temperature measured for the impure alloys of compositions 44.9 and 64.7 at.% Cr in the work of [23Sie] is 1467 °C (Fig. 3).

Solvi

Solid Solubility of Cr in Cu. The solid solubility of Cr in Cu was studied by several authors. Wide discrepancy is present among these results, as shown in Fig. 4 and Table 3. In order to check the relative accuracy between these results, the logarithm of solubility data was plotted against $1/T$ as shown in Fig. 5. The solid solubility of Cu in Cr is known to be negligibly small below the eutectic temperature [Hansen]. Also the solid solubility of Cr in Cu is observed to be less than 1 at.%. Thus, the equilibrium solubility of Cr in the terminal solid solution based on Cu, $X_{Cr}^{(Cu)}$, can be approximated by the equation [68Gor]:

$$\ln X_{Cr}^{(Cu)} = {}^{E}\Delta\overline{S}_{Cr}^{(Cu)}/R - \Delta\overline{H}_{Cr}^{(Cu)}/RT \qquad \text{(Eq 1)}$$

where $\Delta\overline{H}_{Cr}^{(Cu)}$ is the change in enthalpy when 1 mol of Cr with the bcc structure dissolves in Cu to make a dilute solution, (Cu), with the fcc structure, and ${}^{E}\Delta\overline{S}_{Cr}^{(Cu)}$ is the relative partial molar excess entropy of Cr between the (Cr) and (Cu) phases.

The disparity between the different results is reflected in Fig. 5, where the data do not fit into a single straight line.

Table 1 Temperature and Composition Dependence of Liquidus and Solidus

Reference	Composition, at.% Cr	Temperature, °C Liquidus	Solidus
[08Hin]	0.61	···	1077
	1.22	···	1077
	11.96	···	1075
	23.40	···	1075
	34.37	···	1074
	44.90	···	1061
	64.70	···	1063
	83.02	1464	1109
	91.67	1473	1045(?)
[23Sie]	1.22	1079	1076
	2.43	1087	1077
	11.96	1258	1076
	23.40	1326	1078
	34.37	1438	1077
	44.90	1467	1076
	64.70	1470	1075
[57Doi1]	**0.11**	**1084.6**	···
	0.35 to 0.42	**1083.2**	···
	0.68 to 0.70	**1081.9**	···
	1.02	1079.7	···
	1.29	1078.2	···
	1.49	**1077.0**	···
[77Kuz]	2.58	1150	···
	3.86	1220	···
	5.54	1250	···
	8.23	1300	···
[77Kuz](a)	18.1	1400	···
	54.2	1500	···
	79	1600	···
	88	1700	···
	94	1800	···
[82Tim](a)	23.0	1400	···
	27.5	1450	···
	42.0	1550	···

Note: Accepted results are shown in boldface type. All measurements were done by thermal analysis, except those by [77Kuz] done by the solute dissolution method, and the ones by [82Tim] from activity measurements.
(a) Estimated from graph.

Table 2 Eutectic Temperature and Composition

Reference	Temperature, °C	Composition, at.% Cr	Experimental method
[08Hin]	1075	0.61	Thermal analysis
[23Sie]	1076 (1075 to 1078)	1.83 (1.22 to 2.43)	Thermal analysis
[30Cor]	1076	1.52(a)	···
[39Ale]	···	1.1	Optical microscopy
[48Hib1]	1070 ± 2 (1069, 1072)	>1.62	Partially burnt structure
[57Doi1]	**1076.6**	**1.56**	Thermal analysis
[67Zak]	1073 ± 2	0.77	Optical microscopy and X-ray lattice parameter
[77Kuz]	1075	···	Partial dissolution of solute

Note: Accepted results are shown in boldface type.
(a) Extrapolated maximum solubility as estimated by [48Hib1].

The agreement is, however, better at higher temperatures, where equilibrium is more readily attained. The results of [30Cor] are decidedly off. Except for [57Doi1], the data for all other authors deviate from a linear fit at lower temperatures indicating a higher solubility value. This arises due to the difficulty in achieving equilibrium at

Fig. 4 (Cu) Solvus with Selected Experimental Data

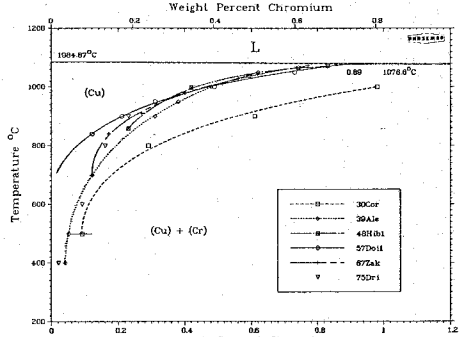

D. J. Chakrabarti and D. E. Laughlin, 1984.

Table 3 Solid Solubility of Cr in Cu

Temperature °C	1000/T(K⁻¹)	Solubility, at.% Cr [30Cor]	[39Ale]	[48Hib1]	[57Doi1]	[67Zak]	[75Dri]
1073 + 2	0.743	···	···	···	···	0.77	···
1069 to 1072	0.745	···	···	0.83 ± 0.09	···	···	···
1066	0.747	···	···	0.74(a)	···	···	···
1050	0.756	···	0.62	···	0.73	···	···
1045	0.759	···	···	0.59(a)	···	···	···
1039	0.762	···	···	0.59(b)	···	···	···
1030	0.767	···	···	···	···	0.56	···
1000	0.786	0.98	0.48	···	0.49	···	···
998	0.787	···	···	0.42(a)	···	···	···
970	0.805	···	···	0.42(b)	···	···	···
950	0.798	···	···	···	···	0.40	···
950	0.818	···	0.38	···	0.31	···	···
910	0.845	···	···	···	···	0.27	···
900	0.853	0.61	0.31	···	0.21	···	0.23
869	0.876	···	···	0.23(b)	···	···	···
858	0.884	···	···	0.23(a)	···	···	···
840	0.898	···	···	···	0.12	0.17	···
800	0.932	0.29	···	···	···	···	0.16
700	1.028	···	0.12	···	···	<0.12	···
600	1.145	···	···	···	···	···	0.09
500	1.294	0.06-0.12	0.05	···	···	···	···
400	1.486	···	0.04	···	···	···	<0.02
Maximum solubility at eutectic temperature:		1.52 (1076)	1.03	0.74-0.92 (1070 ± 2)	0.89 (1076.6)(c)	0.77 (1073 ± 2)	···
Material purity:		?	99.96% Cu 99.8% Cr	? ···	99.99% Cu 99% Cr	99.99% Cu 99.7% Cr	··· ···
Experimental method:		?	Microscopy, chemical analysis	Microscopy(a), electrical resistivity(b)	Microscopy, electrical resistivity	Microscopy, X-ray lattice parameter	Microscopy, chemical analysis

Note: Accepted results are taken from [57Doi1].
(a) Microscopy. (b) Electrical resistivity. (c) Corrected temperature, see text.

Fig. 5 Solubility of Cr in Cu as a Function of Temperature

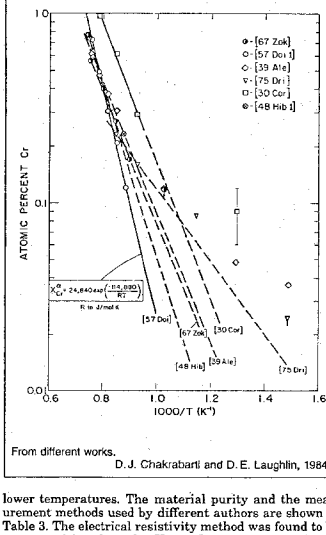

From different works.

D.J. Chakrabarti and D.E. Laughlin, 1984.

lower temperatures. The material purity and the measurement methods used by different authors are shown in Table 3. The electrical resistivity method was found to be more sensitive than the X-ray (lattice parameter), microscopy, or chemical analysis methods [71She]. With microscopy, a higher solubility could be inferred due to the difficulty in observing fine precipitates formed at lower temperatures. Although the data of [57Doi1] do not extend to temperatures as low as those of others, the good linear fit of the results even at temperatures where the rest show deviations, indicate a closer approach to equilibrium in these alloys. The alloys were also made carefully by vacuum melting, using reasonably high-purity material, and were studied by electrical resistivity and microscopy. Although the material used by [75Dri] was even purer, the results, as indicated by a very different slope and deviations of data from a linear plot in Fig. 5, are not acceptable. Therefore, the results of [57Doi1] were used to draw the terminal solubility limits of Cu in Fig. 4. These indicate a much lower level of solubility of Cr in Cu at lower temperatures than considered previously. The equation of the extrapolated line in Fig. 5 from the data of [57Doi1] is:

$$X_{Cr}^{(Cu)} = 24\,840 \exp(-114\,880/RT) \qquad \text{(Eq 2)}$$

where R is in J/mol·K. This equation can be used to calculate the solubility values at (low) temperatures where experimental results are suspect due to lack of equilibrium.

Solid Solubility of Cu in Cr. The solid solubility of Cu in Cr is considered to be negligibly small, but no experimental results are available for the solvus. The only available results pertain to the solidus, and were given by [77Kuz] at two temperatures based on lattice parameter measured by X-ray diffraction. The solubility decreases from 0.16 at.% Cu at 1300 °C to 0.085 at.% Cu at 1150 °C. These results indicate a solidus with a retrograde solubility of Cu in Cr.

Low-Temperature Phase Equilibria

A two-phase equilibrium consisting of the solid solutions based on Cu and Cr exists below the eutectic temperature at all compositions outside the terminal solid solution fields. No intermediate phase has been reported in this system.

Metastable Phases

The Cu-rich (Cu) solid solution alloys are age-hardenable with minimal sacrifice of the electrical conductivity [30Cor, 52Kod, 53Bun, 54Kos]. The precipitates formed are nearly pure Cr. They increase the recrystallization temperature, refine the grain size, and improve the high-temperature strength considerably [39Ale, 48Hib1, 57Doi2, 72Nag]. Electrical conductivity measurements have been used to study the subtle changes during the initial stages of aging. The likelihood of G.P. zone formation in these alloys was ruled out by [75Nag] in view of the absence of an initial increase in resistivity (ρ) at aging temperatures (T_a) below 400 °C. Instead, an abrupt initial drop in ρ occurred, which was interpreted to represent the rapid formation of Cr-rich clusters.

The interpretation of these results is not conclusive. Unless the interparticle distance of the G.P. zones is of the order of magnitude of the mean free path of the conduction electrons, an increase in ρ may not be apparent with the formation of the zones. If the zones form far from one another, the initial resistivity could decrease because of the decreasing amount of solute in the matrix. Thus, the results of [75Nag] do not preclude the formation of G.P. zones.

At T_a above 400 °C, [66Nis1, 73Suz] observed a transient increase in ρ, whose magnitude increased with increasing annealing and decreasing solution temperature. The phenomenon has been related to the reversion or dissolution of clusters formed during aging [54Kos], and the results have been analyzed in terms of the existence of possible metastable phases and their corresponding solvi. [54Kos] could hardly observe any reversion in samples aged at or above 400 °C, while [69Suz] could observe a significant amount of reversion even after aging at 500 °C in a 0.26 % Cr sample. [75Nag] reported the absence of a maximum aging temperature above which reversion could not be observed. From this they inferred the absence of any metastable solvus and, hence, the absence of any metastable phase. [75Nag] employed long aging times to increase the amount of precipitates formed. They also studied the reversion process at short durations (5 s), so as not to miss it in the resistivity drop due to the subsequent precipitation reactions.

Long preaging time, however, can allow the formation of the equilibrium phase and thus, the reversion phenomena

Table 4 Cu-Cr Crystal Structure and Lattice Parameter Data

Phase	Approximate composition range, at.% Cr	Pearson symbol	Prototype	Space group	Lattice parameter, nm a	Comment	Reference
(Cu)	0 to 0.89	*cF4*	Cu	*Fm3m*	0.36147	(a)	[Landolt-Börnstein]
					0.36177	(b)	[52Fal]
(Cr)	99.8 to 100	*cI2*	W	*Im3m*	0.288498 ± 0.000001	(c)	[62Jam]

(a) At 18 °C, on elemental Cu having 0% Cr; indicated composition range of (Cu) corresponds to 1077 °C. (b) On 0.97 at.% Cr-Cu sample quenched rapidly in water from 1600 °C; result as read out from the diagram given by [52Fal]. (c) At 20 °C, on 99.94% pure Cr having impurities, in ppm—O: 500, Fe: 100, N: 3; unfiltered Cu radiation.

studied by [75Nag] could very well correspond to that for the equilibrium phase. The observed reversion effect, in that event, would be due to the capillarity effects [43Kon]. This would also explain the reversion observed during "split aging" [66Nis2, 69Suz] and the gradual decrease in reversion by repeating aging/reversion cycles [66Nis2].

To detect reversion of metastable phases, a short aging time appears essential. This condition appears to have been satisfied in the so-called "step-annealing" employed by [75Nag], involving isothermal annealing in steps of progressively increasing temperature. Under such conditions, two distinct precipitates were observed. The one formed at low temperatures (110 to 260 °C) reverted prior to the onset of the precipitation at the higher temperatures (>350 °C). It is, thus, possible that the precipitates formed at the lower temperatures in step-annealing correspond to the metastable phase, in which case the maxima observed at about 350 °C by [75Nag] for a step-annealing rate of 30 °C/15 min on the 0.28 at.% Cr sample would refer to the metastable solvus temperature.

Regarding the morphology and structure of the initial clusters formed, X-ray studies by [55Gru] and [60Wil] showed ⟨111⟩ streaking on Laue patterns that suggested the formation of thin plates of precipitates (coherent) on the (111) matrix planes. A similar conclusion was reached by [48Hib2]. No separate reflections were observed either in X-ray or in selected area electron diffraction. Thus, the Cr-rich clusters formed initially are not only coherent with the close-packed matrix planes, but appear also to have fcc structure [73Kni]. This suggests the metastable nature of the phase. On longer aging, bcc reflections of Cr do appear that indicate the formation of the equilibrium precipitates.

In conclusion, the evidence used by [75Nag] to suggest the absence of G.P. zones in the Cu-Cr system is not conclusive. On the basis of available results, it rather appears that a fcc Cr-rich metastable phase may indeed form in the initial stages of aging. However, more work is needed to confirm this.

Crystal Structure and Lattice Parameters

The crystal structure and lattice parameter data for Cu and Cr and for the solid solution based on Cu are presented in Table 4. The composition for the solid solution pertains to the supersaturated alloy rapidly (up to 29,000 °C/s) quenched from the melt. The lattice parameter of (Cu) increases linearly with Cr content.

The lattice parameter for Cr was determined from reflections at sufficiently high angles (>80°) for absorption correction to be negligible.

Thermodynamics

Earlier Calculations and Thermodynamic Measurements. Regular solution interaction parameters, denoted by Ω (alternatively, αRT) = ${}^{E}\Delta G/X(1-X)$, were determined by [77Kuz] from the equilibrium between the liquidus and the (Cr) solidus, at 1150 to 1300 °C, and from similar data for the liquid and (Cu) phase [57Doi1]. The interaction parameters thus computed from the phase diagram when applied to higher temperatures indicated that the two-phase equilibria between the liquid and the (Cr) phase persisted over the entire composition range up to pure Cr (Fig. 1). The resultant liquidus is nearly flat in the middle but does not show a miscibility gap. The interaction parameters for the liquid and the (Cr) phase, presented in Table 5 [77Kuz], vary with temperature indicating a departure from the regular solution model in both phases.

Thermodynamic activities of the liquid solution were determined by [82Tim] by high-temperature mass spectrometry between 6 and 97 at.% Cr in the temperature range 1402 to 1616 °C. The results show constant activity values for both Cr and Cu above 42 at.% Cr at 1550 °C. The very large, positive deviation of the activities from ideality for both indicate a strong tendency toward the formation of a miscibility gap in the liquid. The computed activity coefficients of Cr and Cu in the liquid phase at 1550 °C relative to pure liquid Cu and pure solid Cr as standard states are presented in Table 5 (after [82Tim]).

Regular solution interaction parameters for the (Cu) solid solution, $\Omega_{(Cu)}$, was determined by [80Gac] from the excess Gibbs energy of formation of 0.1 at.% Cr-Cu alloy by solid Galvanic cell measurements, and from the equilibrium solubility relations in the phase diagram (after [57Doi1]). The two results presented for 1300 and 1323 K, respectively, in Table 5 show good agreement. The lattice stability parameters from [70Kau] are also included in Table 5.

Estimation of Thermodynamic Parameters from the Phase Diagram. From the limiting slope of the solubility line according to [57Doi1], as accepted in Fig. 5, the partial molar enthalpy of Cr in the (Cu) solid solution, $\Delta\bar{H}_{bcc}^{(Cu)}$ in Eq 1 is determined to be 114.9 kJ/mol. The corresponding value for the partial molar entropy, ${}^{E}\bar{S}_{bcc}^{(Cu)}$, from the intercept of the extrapolated solubility line at $X_{Cr}^{(Cu)} = 108$, is calculated to be 38.95 J/mol·K. The enthalpy and entropy of transformation of Cr from bcc → fcc, as obtained from [70Kau] and assumed to be independent of temperature, are 10.46 kJ/mol and −0.63 J/mol·K, respectively. From the above results, the values for the corresponding differential heat of solution (relative partial molar enthalpy), $\Delta\bar{H}_{Cr}^{(Cu)}$, and the differential entropy of solution (relative partial molar excess entropy), ${}^{E}\Delta\bar{S}_{Cr}^{(Cu)}$,

Table 5 Thermodynamic Parameters of Different Phases

Parameter, J/mol	Liquid	Phase (Cr)	(Cu)
Interaction parameter(Ω)	88 533 − 35.56 T (a) 30 645(c)	99 998 − 34.10 T (a)	43 400(b) 43 000 + 13.000$\dot{d}$) 20 000 − 7.0 T (e)
	81 200 + 4 400 X_{Cr} −27.9 T (f)	...	19 860 − 7.0 T −0.024(T − 1223)^2(g)
RT ln γ_{Cr}	8.45RT(1 − X^l_{Cr})^2(h)	...	...
RT ln γ_{Cu}	8.45RT(1 − X^l_{Cr})^3 + 0.79	...	...
Relative partial molar enthalpy, $\Delta\bar{H}^{(Cu)}_{mCr}$	...	...	104 430(j)
Partial molar excess entropy, $^E\Delta\bar{S}^{(Cu)}_{mCr}$	...	...	39.58 (J/mol·K)(j)
Lattice stability parameters (k)			
$F^{l\to fcc}$	...	−7 740 + 9.0 T	−13 054 + 9.62 T
$F^{fcc\to bcc}$	...	−10 460 − 0.63 T	3 556 − 0.84 T
$F^{l\to bcc}$	...	−18 200 + 8.37 T	−9 498 + 8.79 T
Molar free energy of fusion (m)	...	7 692 + 142.97 T +7.766 × 10^{-3} T^2 −8.3492 × 10^5 T^{-1} −21.260 T ln T	7 683 + 38 844 T +1.8933 × 10^{-2} T^2 −6.527 T ln T

(a) [77Kuz]. (b) [80Gac] at 1323 K from the phase diagram. (c) This evaluation, from activity data of Cu in liquid at 1823 K by [82Tim]. (d) [80Gac] at 1300 K from Calvanic measurements. (e) This evaluation, for 1113 to 1223 K. (f) This evaluation. (g) This evaluation, for 1223 to 1322 K. (h) [82Tim] at 1823 K. (j) This evaluation; from solubility data. (k) [70Kau]. (m) [77Bar].

Table 6 Composition vs Interaction Parameters of Cu and Cr In Liquid at 1823 K

Composition, X_{Cr}	Interaction parameters, J/mol Ω^l_{Cr}	Ω^l_{Cu}	Composition dependence of Ω^l_i, J/mol
0.1....	33 800 ± 3 200	30 000 ± 15 000	
0.2....	34 200 ± 3 600	29 200 ± 6 900	Ω^l_{Cr} = 6070 X_{Cr} + 33 100
0.3....	34 800 ± 3 000	30 700 ± 5 500	
0.4....	35 600 ± 2 300	30 500 ± 5 400	Ω^l_{Cu} = 6070 X_{Cu} + 28 000
0.42...	35 800 ± 2 000	30 700 ± 5 300	

Note: From activity data for liquid at 1823 K by [82Tim], modified to be relative to the standard states of pure liquid Cu and and pure liquid Cr.

are calculated to be 104.43 kJ/mol and 39.58 J/mol·K, respectively. The results are presented in Table 5, where αCr and βCr refer to Cr with fcc and bcc structures, respectively.

A temperature dependence of Ω_{Cu} was calculated from the Cu-Cr equilibrium diagram after [80Gac], based on the following relationship:

$$\Omega = [RT(\ln X^{(Cr)}_{Cr} - \ln X^{(Cu)}_{Cr}) - \Delta G^{(Cr)\to(Cu)}_{Cr}] / [1 - X^{(Cu)}_{Cr}]^2 \quad \text{(Eq 3)}$$

where $X^{(Cr)}_{Cr}$ and $X^{(Cu)}_{Cr}$ stand for mole fractions of Cr in the (Cr) and (Cu) phases, respectively, and $\Delta G^{(Cr)\to(Cu)}_{Cr}$ is the stability parameter for Cr for transformation from bcc to fcc structure. The results are presented in Table 5. The Ω at 1550 °C calculated from the ln γ expression for Cu [82Tim] is included in Table 5 for comparison.

The large $\Delta\bar{S}^{(Cu)}_{mCr}$ value calculated earlier indicates the (Cu) phase to deviate considerably from Hildebrand's model of regular solution [29Hil].

Thermodynamic Calculations. The interaction parameters, Ω, used by [77Kuz] for the calculation of the liquidus were derived from their phase diagram results alone and did not incorporate any composition dependence effects. An attempt has been made in this evaluation to take into account both the activity data of the liquid by [82Tim] and the aforementioned liquidus and solidus data by [77Kuz],

Fig. 6 Interaction Parameters of Cu and of Cr in the Liquid as a Function of Composition

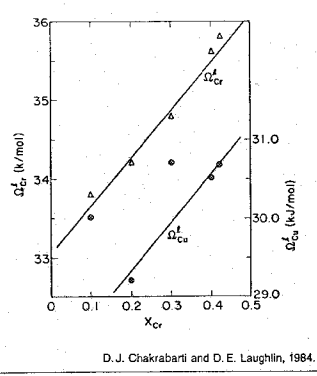

to derive an optimized expression for the interaction parameter of the liquid, Ω^l, that incorporates both the temperature (T) and composition (X) dependence. Using this expression, the equilibrium liquidus is calculated.

In order to determine the composition dependence of Ω for Cr in the liquid, Ω^l_{Cr}, the partial molar excess free energy values for Cr, $^E\Delta\bar{G}^l_{Cr}$, derived from the activity data of [82Tim], were modified to correspond to those relative to the liquid as standard states for both components. The variation of the resultant Ω^l_{Cr} with composition is shown in Fig. 6 and Table 6. The values of Ω^l_{Cu} were also calculated

Fig. 7 Interaction Parameters of Cu and of Cr in the Liquid as a Function of Temperature

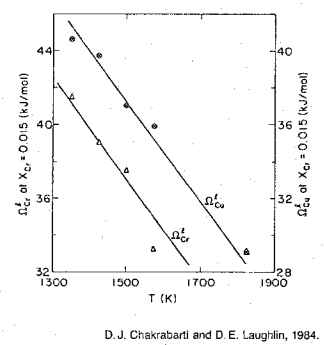

D.J. Chakrabarti and D.E. Laughlin, 1984.

from the composition of the liquid in equilibrium with the (Cr) phase, assuming the solid solution as Raoltian. The values were modified to correspond to the eutectic composition at X_{Cr} = 0.0156, based on the composition dependence derived as in Table 6. The resultant Ω^l_{Cr} values as a function of temperature are shown in Fig. 7 and Table 7. The combined T and X dependence of Ω^l_{Cr} is presented in Table 7.

The Ω^l_{Cu} values were derived from the above expression of Ω^l_{Cr} by the application of the Gibbs-Duhem relation for the temperature-dependent part (Fig. 7 and Table 8) and directly from the $^{E}\Delta\bar{G}^l_{Cu}$ values of [82Tim] for the composition-dependent part (Fig. 6 and Table 6). The variation of Ω^l_{Cu}, with T and X is shown in Table 8. The resultant integral expression for Ω^l is as follows:

$$\Omega^l = X_{Cu} \cdot (1 - X_{Cr}) \cdot (81\,200 + 4\,400\,X_{Cr} - 27.9\,T) \quad \text{(J/mol)} \qquad \text{(Eq 4)}$$

The free energy of fusion for Cr, ΔG^f_{Cr}, was derived from [77Bar] and is as follows (see Table 5, for the corresponding expression for Cu):

$$\Delta G^f_{Cr} = 7692 + 142.97\,T + 7.766 \times 10^{-3}\,T^2 - 8.3492 \times 10^5\,T^{-1} - 21.260\,T \ln T \quad \text{(J/mol)} \qquad \text{(Eq 5)}$$

Based on the above expression of Ω^l for the liquid and assuming a simple Henrian solution for the (Cr) phase, the resultant liquidus as well as its metastable miscibility gap at lower temperatures were calculated and are presented in Fig. 3. The calculations clearly demonstrate that the liquid develops a miscibility gap that lies just below the liquidus. This would account for the large flat portion of the liquidus in the midcomposition region. This also explains the several observations of the liquid miscibility gap by early investigators, in that small amounts of impurities may be sufficient to stabilize the gap.

The calculated liquidus, however, is shifted upward from the liquidus based on the experimental data of [77Kuz] and [82Tim]. This may be the consequence of the inherent approximations involved in deriving the expression for Ω^l. However, the information regarding the relative position of the miscibility gap with respect to the liquidus is still valid.

Table 7 Interaction Parameters of Cr in Liquid vs Temperature

$\Omega^l_{Cr} = 81\,200 + 6070\,X_{Cr} - 27.9\,T$

Temperature, K	Interaction parameters, J/mol Ω^l_{Cr}	X_{Cr}	$\Omega^l_{Cr}(X^l_{Cr} = 0.015)$, J/mol
1350	41 500	0.015	41 500
1423	38 950	0.026	39 000
1498	37 300	0.040	37 500
1573	32 800	0.082	33 200
1823	···	···	33 100

Note: Calculations using phase diagram results by [77Kuz], and for T = 1823 K, activity results by [82Tim].

Table 8 Interaction Parameters of Cu in Liquid vs Temperature

$\Omega^l_{Cu} = 79\,500 + 6070\,X_{Cr} - 27.9\,T$

Temperature, K	Interaction parameters, J/mol Ω^l_{Cu}	X_{Cr}	$\Omega^l_{Cu}(X^l_{Cr} = 0.015)$, J/mol
1350	40 600	0.015	40 600
1423	39 650	0.026	39 700
1498	36 600	0.040	37 000
1573	34 700	0.082	35 900
1823	···	···	29 100

Note: From Table 7 by applying Gibbs-Duhem Relation and, for T = 1823 K, from activity results by [82Tim].

Suggestions for Future Experimental Work

Critical experimentation is needed to determine if, in the absence of impurities, the equilibrium miscibility gap in the liquid in Cu-Cr alloys is merely diminished in area, as in the Cu-V system [81Smi], or if it indeed disappears, as in the Cu-Nb system [78Ver].

Cited References

06Gui: L. Guillet, "Recent Researches on Alloys of Industrial Importance", *Rev. Met., 3*, 176 (155-179), (1906) in French. (Equi Diagram; Experimental)

08Hin: G. Hindrichs, "Some Cr and Mn Alloys", *Z. Anorg. Chem., 59*, 420-423 (414-449), (1908) in German. (Equi Diagram; Experimental; #)

*23Sie: E. Siedschlag, "Cr-Cu-Ni Alloys", *Z. Anorg. Chem., 132*, 173-178 (173-190), (1923) in German. (Equi Diagram; Experimental; #)

29Hil: J.H. Hildebrand, "Solubility XII, Regular Solutions", *J. Am. Chem. Soc., 51*, 66-80 (1929). (Therme; Theory)

30Cor: M.G. Corson, "Cu Alloy Systems with α-Phase Having Variable Limits and Their Use for Hardening of Cu", *Rev. Met., 27*, 83-95 (1930) in French. (Equi Diagram; Experimental)

39Ale: W.O. Alexander, "Annealing Characteristics and Solid Solubility Limits of Cu and Cu Alloys Containing Cr", *J. Inst. Met., 64*, 93-109 (1939). (Equi Diagram; Experimental)

42Kon: S.T. Konobeevski, "A Thermodynamical Theory of Restoration Phenomena in Aging of Cu-Al Alloys", *J. Inst. Met., 69*, 397-413 (1943). (Thermo, Meta Phase; Theory)

48Hib1: W.R. Hibbard, Jr., F.D. Rosi, H.T. Clark, Jr., and R.I. O'Herron, "The Constitution and Properties of Cu-Rich Cu-Cr and Cu-Ni-Cr Alloys", *Trans. AIME, 175*, 283-294 (1948). (Equi Diagram; Experimental)

48Hib2: W.R. Hibbard and N.K. Chen, "Metallographic Observations of Precipitation in Cu-Cr Alloys", *Trans. AIME, 175*, 294-295 (1948). (Equi Diagram; Experimental)

52Fal: G. Falkenhagen and W. Hofman, "Influence of High Cooling Rates on Solidification and Structure of Binary Alloys", *Z. Metallkd., 43*, 69-81 (1952) in German. (Crys Structure; Experimental)

52Kod: S. Koda and E. Isono, "On Heat-Treating Cu-Cr Alloy", *J. Jpn. Inst. Met., 16*(4), 213-217 (1952) in Japanese. (Equi Diagram; Experimental)

53Bun: G. Bunge, E.R. Honak, and W. Nielsch, "Properties of Technically Useful Cu-Cr Alloys", *Z. Metallkd., 44*, 71-76 (1953) in German. (Equi Diagram; Experimental)

*54Kos: W. Koster and W. Knorr, "Property Changes During Annealing in Cu-Cr Alloys", *Z. Metallkd., 45*, 350-356 (1954) in German. (Equi Diagram, Meta Phase; Experimental)

55Gru: W. Gruhl and R. Fischer, "Hardening and Deformation in Cu-Cr", *Z. Metallkd., 46*(10), 742-748 (1955) in German. (Equi Diagram; Experimental)

*57Doi1: T. Doi, "Studies on Cu Alloys Containing Cr (1st Report). On the Cu Side Phase Diagram", *J. Jpn. Inst. Met., 21*(5), 337-340 (1957) in Japanese. (Equi Diagram; Experimental; #)

*57Doi2: T. Doi, "Softening and Age-Hardening of Cu Alloys Containing Cr", *J. Jpn. Inst. Met., 21*(12), 720-724 (1957) in Japanese. (Equi Diagram; Experimental)

60Wil: R.O. Williams, "Precipitation Process in Cu-Cr Alloys", *Trans. ASM, 52*, 530-544 (1960). (Equi Diagram; Experimental)

62Jam: W.J. James, M.E. Straumanis, and P.B. Rao, "Anomaly in Expansivity Curve of Cr", *J. Inst. Met., 90*, 176-177 (1962). (Crys Structure; Experimental)

66Nis1: S. Nishikawa, K. Nagata, and S. Kobayashi, "On Aging Process of Cu-Cr Alloys", *J. Jpn. Inst. Met., 30*(3), 302-307 (1966) in Japanese. (Equi Diagram; Experimental)

66Nis2: S. Nishikawa, K. Nagata, and S. Kobayashi, "On Reversion Phenomena of Cu-Cr Alloys", *J. Jpn. Inst. Met., 30*(8), 760-765 (1966) in Japanese. (Meta Phase; Experimental; #)

67Zak: M.V. Zakharov and O.E. Osintsev, "Phase Diagram of Cu Corner of Cu-Cr-Ni System", *Izv. Vyssh. Ucheb. Zaved., Tsvetn. Met., 5*, 152-155 (1967) in Russian. (Equi Diagram; Experimental)

68Gor: P. Gordon, *Principles of Phase Diagrams in Materials Systems*, McGraw-Hill, New York, 142-145 (1968). (Thermo; Review)

69Suz: H. Suzuki, H. Kitano, and M. Kanno, "Reversion Phenomena in Cu-Zr-Cr Alloys", *J. Jpn. Inst. Met., 33*(3), 334-338 (1969) in Japanese. (Equi Diagram, Meta Phase; Experimental)

70Kau: L. Kaufman and H. Bernstein, *Computer Calculations of Phase Diagrams*, Academic Press, New York, 184-185 (1970). (Thermo; Compilation)

71Shc: V.F. Shchirin, V.M. Rosenberg, and N.P. Belousov, "Determining Concentration of Solid Solution of Cr Bronze from Magnitude of Electrical Resistance", *Tsvetn. Met., 12*, 74 (1971) in Russian; TR: *Sov. J. Non-Ferrous Met., 12*, 85 (1971). (Equi Diagram: Experimental)

72Nag: T. Nagai, Z. Henmi, T. Sakamoto, and S. Koda, "Effect of Size of Precipitates on Recrystallization Temperature in Cu-Cr, Cu-Zr, and Cu-Zr-Cr Alloys", *J. Jpn. Inst. Met., 36*(6), 564-571 (1972) in Japanese. (Equi Diagram; Experimental)

73Kni: R.W. Knights and P. Wilkes, "Precipitation of Cr in Cu and Cu-Ni Base Alloys", *Met. Trans., 4*(10), 2389-2393 (1973). (Equi Diagram; Experimental)

73Suz: H. Suzuki and M. Kanno, "Initial Aging Phenomena in Cu-Cr Alloy", *J. Jpn. Inst. Met., 37*(1), 13-18 (1973) in Japanese. (Equi Diagram, Meta Phase; Experimental)

75Dri: M.E. Drits, L.L. Rokhlin, N.R. Bochvar, E.V. Lysova, V.M. Rozenberg, A.K. Nikolaev, and N.B. Shparo, "Solubility of Cr and Hf in Cu Solid State", *Izv. Vyssh. Ucheb. Zaved., Tsvetn. Met., 2*, 122-125 (1967) in Russian; TR: *Sov. Non-Ferrous Met. Res., 2*, 74-76 (1975). (Equi Diagram; Experimental)

*75Nag: K. Nagata and S. Nishikawa, "Aging and Reversion Phenomena of Cu-Cr Alloy", *Rept. Inst. Indust. Sci., Univ. of Tokyo, 24*(4), Serial No. 153, 115-168 (Mar 1975). (Equi Diagram; Meta Phase; Experimental)

77Bar: I. Barin, O. Knacke, and O. Kubaschewski, *Thermochemical Properties of Inorganic Substances* (1973), and Supplement, Springer-Verlag, NY (1977). (Thermo; Compilation)

*77Kuz: G.M. Kuznetsov, V.N. Fedorov, and A.L. Rodnyanskaya, "Investigation of Phase Diagrams of Cu-Cr System", *Izv. Vyssh. Ucheb. Zaved., Tsvetn. Met., 3*, 84-86 (1977) in Russian; TR: *Sov. Non-Ferrous Met. Res., 3*, 104-105 (1977). (Equi Diagram, Thermo; Experimental; #)

78Ver: J.D. Verhoeven and E.D. Gibson, "The Monotectic Reaction in Cu-Nb Alloys", *J. Mater. Sci., 13*, 1576-1582 (1978). (Equi Diagram, Meta Phase; Experimental)

81BAP: *Bull. Alloy Phase Diagrams, 2*(1), 146 (1981), for melting point of elements corrected to conform to the 1968 ITPS scale. (Equi Diagram; Compilation)

81Smi: J.F. Smith and O.N. Carlson, "The Cu-V System", *Bull. Alloy Phase Diagrams, 2*(3), 348-351 (1981). (Equi Diagram; Compilation)

82Cha: D.J. Chakrabarti and D.E. Laughlin, "The Cu-Nb System", *Bull. Alloy Phase Diagrams, 2*(4), 455-460 (1982). (Equi Diagram, Meta Phase; Review)

*82Tim: L. Timberg and J.M. Toguri, "A Thermodynamic Study of (Copper + Chromium) by Mass Spectrometry", *J. Chem. Thermodyn., 14*, 193-199 (1982). (Thermo, Equi Diagram; Experimental; #)

*Indicates key paper.

Reference contains data used in drawing the accepted phase diagram.

Cr-Cu evaluation contributed by D.J. Chakrabarti and D.E. Laughlin, Department of Metallurgical Engineering and Materials Science, Carnegie-Mellon University, Pittsburgh, PA 15213, USA. Work was supported by the International Copper Research Association, Inc. (INCRA), and the Department of Energy through the Joint Program on Critical Compilation of Physical and Chemical Data coordinated through the Office of Standard Reference Data (OSRD), National Bureau of Standards. Thermodynamic calculations were done in part with the use of the F*A*C*T computer program, made available to us by Drs. A.D. Pelton, W.T. Thompson, and C.W. Bale of McGill University/Ecole Polytechnique. Literature searched through 1982. Professor Laughlin and Dr. Chakrabarti are the ASM/NBS Data Program Co-Category Editors for binary copper alloys.